

DEVELOPMENT AND EVALUATION OF AN ULTRASONIC GROUNDWATER SEEPAGE METER

Ronald J. Paulsen

*Suffolk County Health Services - Bureau of Water Resources
225 Rabro Dr., Hauppauge NY 11788*

Christopher F. Smith

*Cornell Cooperative Extension of Suffolk County - Marine Program
3059 Sound Ave., Riverhead, NY 11901*

Teng-fong Wong

*Department of Earth and Space Sciences, State University of New York at Stony Brook
Stony Brook, NY 11794-2100*

Abstract

A continuously recording groundwater seepage meter was developed using ultrasonic flow detection technology. A commercially available ultrasonic flowmeter was adapted to a 10''-diameter collection funnel and utilized to measure groundwater underflow to tidal surface waters. The difference between upstream and downstream transit times is directly proportional to the flow rate. Testing and calibration runs were performed in a specially designed water tank, and the data show that seepage rates on the order of 10^{-6} cm/s can be resolved. Reverse flow can also be detected and measured with this technique. The seepage meter was deployed in Coecles Harbor, Long Island, New York. Seepage rates and tidal stages were recorded simultaneously. The data clearly show a negative correlation between the seepage rate and tidal stage. The upper glacial aquifer was modeled as an anisotropic, unconfined aquifer and the complex variable technique was used to calculate the flow net and submarine specific discharge at the seepage surface. The theoretical predictions are in reasonable agreement with field observations on the water table, fresh-salt water interface, as well as evolution of seepage rate with the tidal cycle.

Introduction

Groundwater can flow directly into the sea through porous rocks and sediments. It seeps from unconfined aquifers into the near shore or is discharged from confined aquifers found underneath continental shelves further from shore. According to Church (1996), previous estimates of the amount of this submarine groundwater discharge worldwide range from 0.01 to 10% of surface-water runoff. A better quantification has been difficult because there is a paucity of direct measurements of submarine groundwater discharge. Indirect inference of the discharge is difficult because of insufficient information on hydraulic gradients and transmission coefficients along the world's coasts.

The conventional method for measurement of groundwater seepage was designed by Israelsen and Reeve (1944) and Lee (1977). In this method, the open, cut-off end of a 55-gallon steel drum is pushed into the bottom sediment. A plastic bag attached to a tube in the top of the drum catches seepage water after it passes through the drum and into the tube. The groundwater

head of the adjacent upland area induces the fresh groundwater to seep into the drum funnel. After a period of time, the bag is removed from the tube and the collected volume of water measured. Dividing this volume by the time deployed and the area covered by the funnel enables a measurement of seepage rate. Although crude, this technique produced the first direct measurements of groundwater seepage and has been successfully applied in various hydrogeologic settings, including lakes, reservoirs, rivers, estuaries and coasts. Bokuniewicz (1980) used this method on Long Island to investigate the groundwater seepage into the Great South Bay.

Recent studies (e.g. Carr and Winter, 1980; Shaw and Prepas, 1989 and 1990; Taniguchi and Fuko, 1993; Cherkauer and McBride, 1988; Fukuo, 1991) have underscored certain limitations of the drum method, including the labor-intensive nature of its deployment, the time required to gain enough experience to determine how long to deploy a meter at a certain location, the potential for the plastic bag to influence water flow, the lack of accuracy at low seepage flows, and the inability to continuously log flow data. Accordingly seepage meters have been developed that overcome some of these limitations. Taniguchi and Fukuo (1991) developed a seepage meter based on a heat pulse method. It can continuously measure and record seepage rates. Cherkauer and McBride (1988) developed a remotely deployed meter. However, it requires a large vessel and can not be used in shallow water depths. Walthall and Reay (1993) developed a remotely deployable meter that has been used in Chesapeake Bay.

Description of Device

In recent years ultrasonic flow meters have been developed and used to measure relatively low flow rates in a variety of water and wastewater industries. In this study we take advantage of this advancement in ultrasonic technology to develop a seepage meter for continuous measurement of submarine groundwater discharge.

A transient-time flow meter uses the effect of the flow on the travel time of an ultrasonic signal as the bases for determining the flow rate.

Figure 1 shows a cross section of the meter with

the path of the flow tube sonic beam and non-intrusive transducers. A multi-pulse sonic signal is transmitted through the flow tube in both directions by transducers located at opposite ends. When there is no flow the signal will arrive at each transducer at the same time. However, when there is flow in the tube the upstream flow will cause the signal to arrive ahead of the signal traveling downstream. The difference in transit times (Δt) between the two signals is proportional to the liquid's flow velocity V_f . The constant of proportionality depends on the average of the upstream and downstream transit times and length L of the tube. The specific discharge from the seepage surface q is inferred from the flow velocity by multiplying V_f by the ratio between the areas of the flow tube and the collection funnel.

Our seepage meter system is based on the widely used technique of placing a funnel into the seepage surface on the seabed to capture submarine groundwater discharge (Figure 2). This

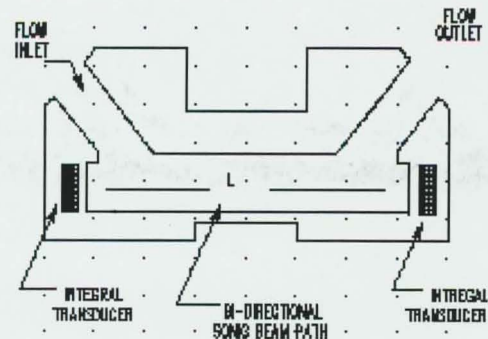


Figure 1. Cross section of ultrasonic flowmeter.

seepage flow is then directed via tubing through the ultrasonic meter which is connected to a data logger. The sampling frequency and duration are programmed into the logger by the investigator. This meter can detect reversals in flow, and it includes a totalizer which acquires data on cumulative volume of water passing through the meter which (when after normalized by the collection funnel area) provides the specific discharge. Our prototype funnel (collection device) is 10" in diameter, corresponding to an area of 5067.07 cm².

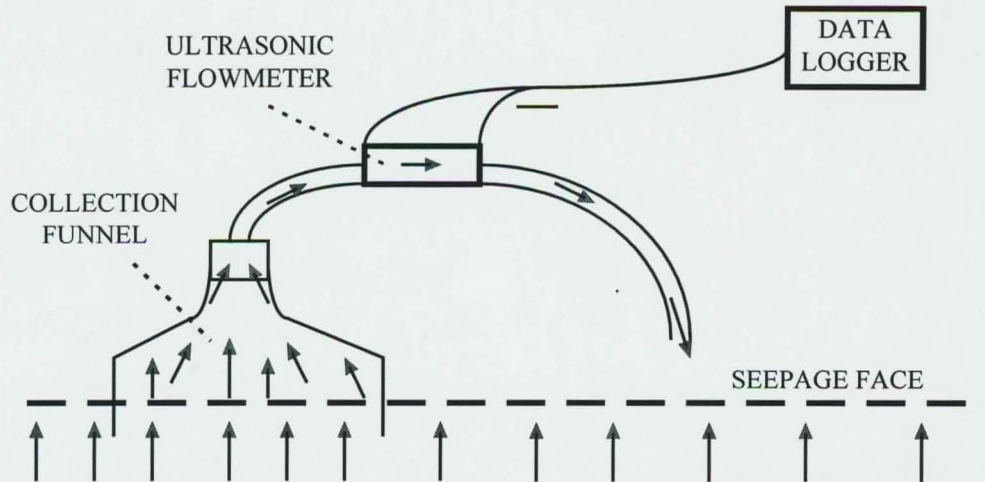


Figure 2: Diagram of ultrasonic flowmeter installation on the seabed. Arrows indicate flow of seepage water into the collection funnel that has been placed in the seabed.

Calibration

A calibration exercise was completed at the Suffolk County Marine Environmental Learning Center at Cedar Beach, New York. The calibration system consisted of an elevated constant head tank connected to an experimental seepage tank (Figure 3). A manifold constructed of ½" PVC pipe was placed in the bottom of this tank. The manifold was connected via hose to the constant head tank. Holes were drilled in the manifold to distribute water flow throughout the bottom of the tank, and a 8" layer of small rock was placed on top of the manifold. In addition, a 24" layer of beach sand was placed on top of the rock layer. The flow rate was controlled by a valve in the hose from the constant-head tank.

The collection funnel of the seepage meter was pushed carefully into the sand. After passing through the meter the flow is directed outward and downward by a short length of hose. The cumulative discharge was measured simultaneously by the ultrasonic flow meter using the totalizer and by a graduated cylinder at the terminus of the bulkhead connected to the meter outflow hose. To inhibit the development of hydraulic gradient in the calibration tank and to ensure that the flow through the funnel encounters no head resistance, excess flow into the calibration tank is allowed to exit the tank through a separate bulkhead drain.

A detailed description of the calibration procedure and results will be presented by Paulsen and Smith (1997). Independent measurements from the ultrasonic flow meter and the graduated cylinder confirmed the linearity of the seepage meter. It can resolve relatively low seepage rates on the order of 10^{-6} cm/sec ($V_f = 0.05$ cm/sec). Our calibrations for a collection funnel of 10" diameter showed that a seepage rate $q = 2.96 \times 10^{-5}$ cm/sec results in a flow

velocity $V_f = 0.15$ cm/sec. A higher resolution can be attained by enlarging the area of the collection funnel. Several designs have recently been tested, including a funnel with a square cross-section of dimensions 24" x 24".

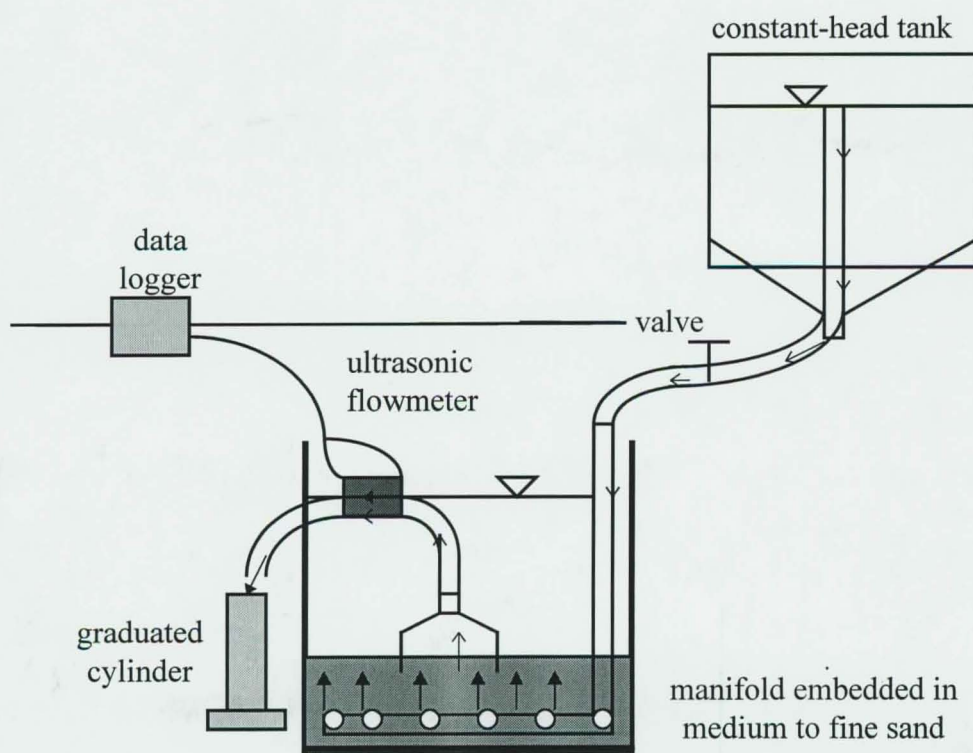


Figure 3. Calibration tank setup showing the positions of the constant-head system, graduated cylinder and ultrasonic flowmeter.

Field Deployment

Following the calibration test our seepage unit was tested in the field at a known seepage interface on Shelter Island. It was deployed from a dock at St. Gabriel's Retreat House in the vicinity of the USGS well transect terminating at Coecl's Harbor (Figure 4). This dock

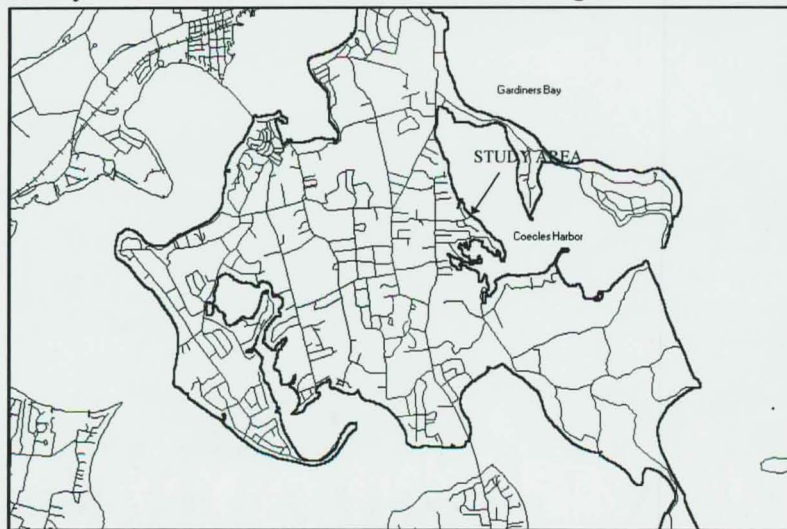


Figure 4- Location of meter field deployment in Coecl's Harbor, Shelter Island.

conveniently passes across the interface and has the requisite electric power to drive the unit. Also deployed at the dock was a continuously logging tide gauge which enabled the comparison of tidal height and seepage flow rate. In order to verify that the funnel was receiving fresh water and not recirculated seawater, grab samples were taken from the outlet of the flowmeter. The electric conductivities of these grab samples were characterized in the laboratory.

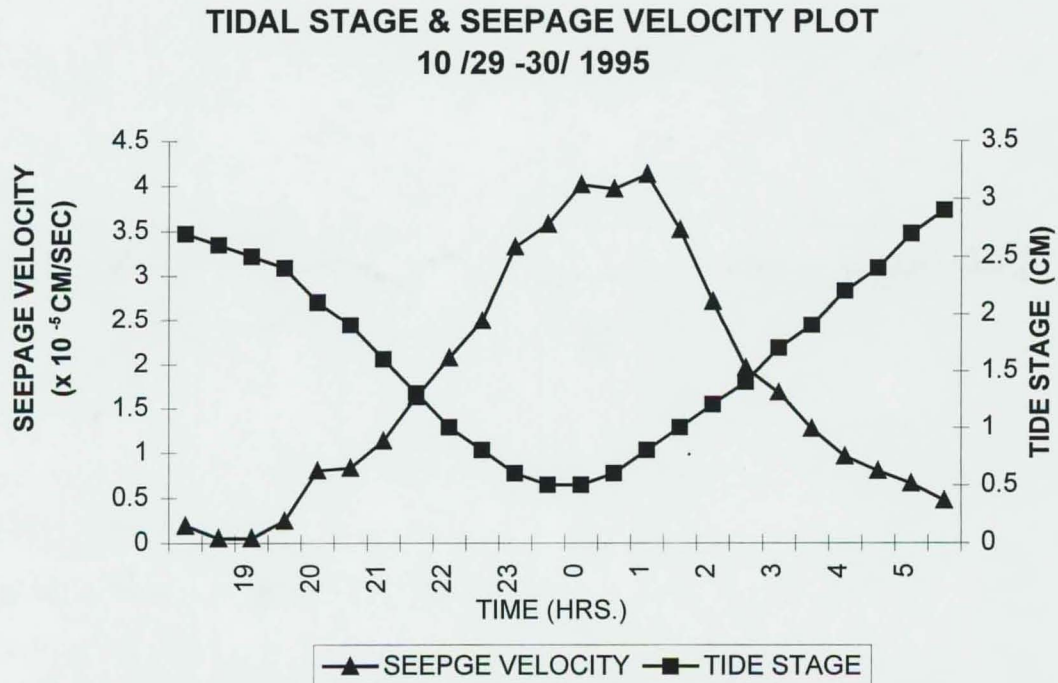


Figure 5. Plot of tidal stage and seepage rates in Coecles Harbor, New York

Figure 5 is a set of representative data of tidal height and seepage flow velocity as functions of time. This data reveal a negative correlation between tidal height and seepage velocity. The negative correlation between tidal stage and seepage velocity can be qualitatively explained by the elevation of the hydraulic potential of the sea water by high tides which would inhibit the submarine discharge of fresh groundwater out of the seepage surface. In the next section, we will introduce a flow model to quantitatively explain the negative correlation.

Other investigators have hypothesized that rainfall could influence seepage directly, and wind could influence seepage indirectly by influencing tidal height. Statistical correlation of these factors with seepage velocity will be investigated in the future. The range of flow rates through the flowmeter were from 0 to 0.2 cm/sec which correlates to a specific discharge of 0 to 3.94×10^{-5} cm/sec. Generally, peaks in flow occurred around 0.15 cm/sec. The total volume of water passing through the meter over any portion of the graph is displayed in the spreadsheet. For the tidal cycle on 10/29-30/94 this volume was 27 cc over the area of the funnel. This equates to 483 cc per tidal cycle per square meter, or almost 1 liter per day per square meter.

Electric conductivity of the grab samples ranged from 400 to 1200 micromhos/cm. Since the saltwater of Coecles Harbor had values of 35,000 micromhos/cm, we conclude that the seepage was from fresh underground water. Thus, it can be concluded that at this portion of the interface very little recirculation of saltwater occurring, as discussed in Cooper et al. (1964). We are exploring the feasibility of continuously monitoring the salinity of seepage water by inferring it from the sonic velocity measured in the flow tube of the seepage meter (Paulsen and Smith, 1997). There is a one-to-one correspondence between sonic velocity and salinity at a given temperature of water.

Salt water encroachment in an anisotropic, unconfined aquifer

Freshwater on Shelter Island flows from high water table areas to the perimeter shore line area where it will interface with saltwater. When fresh groundwater meets denser sea water in a coastal aquifer, the fresh water will tend to float on the sea water. The Ghyben-Herzberg principle is often used to describe the nature of the salt/fresh water interface:

$$Z = Gh \quad \text{with} \quad G = \frac{\rho_w}{\rho_s - \rho_w} \quad (1)$$

where Z = depth to salt water interface below MSL (Mean Sea Level), h = elevation of water table above MSL, ρ_s = density of saltwater and ρ_w = density of fresh water. This simple relation is based on two key assumptions: hydrostatic conditions must prevail in both freshwater wedge and sea water, and there is a sharply defined interface between fresh and saltwater.

The first assumption is relaxed in the Dupuit-Ghyben-Herzberg model (Fetter, 1972). The freshwater wedge is not in hydrostatic equilibrium, and the dynamic flow in the aquifer is described by the Dupuit approximation. However, this dynamic model has the limitation that the saltwater interface is predicted to intercept the water table at the coastline, and therefore the submarine underflow at the near shore is not accounted for. To circumvent this limitation, several models were developed using complex variable theory. The simplest results were derived by Glover (1964) for a water wedge which is isotropic and confined. However, the fresh water in our study area is located in the upper glacial aquifer which is unconfined and anisotropic. Such a hydrological setting was analyzed by Rumner and Shiao (1968) using the theory of complex variable and analytic function.

Consider an unconfined aquifer with vertical and horizontal hydraulic conductivities given by K_z and K_x respectively. The upper boundary of the aquifer is given by the water table with a slope such that the flow occurs along a subhorizontal direction. The average discharge (per unit width of the aquifer) is denoted by Q and a coordinate system is defined with the origin located at the intersection of the water table with the coast line. The Z -axis points vertical downward into the aquifer, and the X -axis runs from the coastline in a horizontal, landward direction. Rumner and Shiao's (1968) theory predicts that the locations of the water table and fresh-salt interface are respectively given by:

$$Z^2 = \frac{2Q}{\sqrt{K_x K_z} (G+1)} X \quad (2a)$$

$$Z^2 = \frac{2QG^2}{\sqrt{K_x K_z} (G+1)} X + \frac{Q^2}{K_z^2} \frac{G^2(G-1)}{G+1} \quad (2b)$$

According to these two equations, the water table and fresh-salt water interface are controlled by two independent parameters: $Q / \sqrt{K_x K_z}$ and Q / K_z , or equivalently in terms of

$Q / \sqrt{K_x K_z}$ (which is related to the average hydraulic gradient in the unconfined aquifer) and K_x / K_z (which characterizes the anisotropy of the hydraulic conductivity). Using water table data for 5 wells (extending from 30' to 2,000' from the average tide mark on the coast) along the transect, we applied linear regression (to equation (2a) with Z^2 and X as the dependent and

independent variables) to infer $Q / \sqrt{K_x K_z}$ to be $\sim 0.044'$. Furthermore, preliminary well log data (on electrical conductivity and salinity as functions of depth) together with equation (2b) constrain the anisotropy ratio $K_x / K_z \approx 40$. Using these parameters, the flow net (Figure 6) can be calculated according to

$$X = \frac{Q}{\sqrt{K_x K_z}} \frac{K_x}{K_z} \left[\frac{G+1}{2} (\Phi^2 - \Psi^2) - \Psi \right] \quad (3a)$$

$$Z = \frac{Q}{\sqrt{K_x K_z}} \frac{K_x}{K_z} [(G+1)\Phi\Psi + \Phi]. \quad (3b)$$

where Ψ and Φ are the stream function and potential function respectively. When Ψ is constant stream lines are mapped out in the X - Z plane by the above equations. The upper boundary (water table) is defined by $\Psi = 0$, and the fresh-salt water interface by $\Psi = -1$. The other stream lines are mapped out by constant values Ψ between -1 and 0. Similarly the equipotential lines are contoured by holding the potential function Φ constant at various values between -1 and 0 with $\Phi = 0$ corresponding to the seepage face (Figure 6).

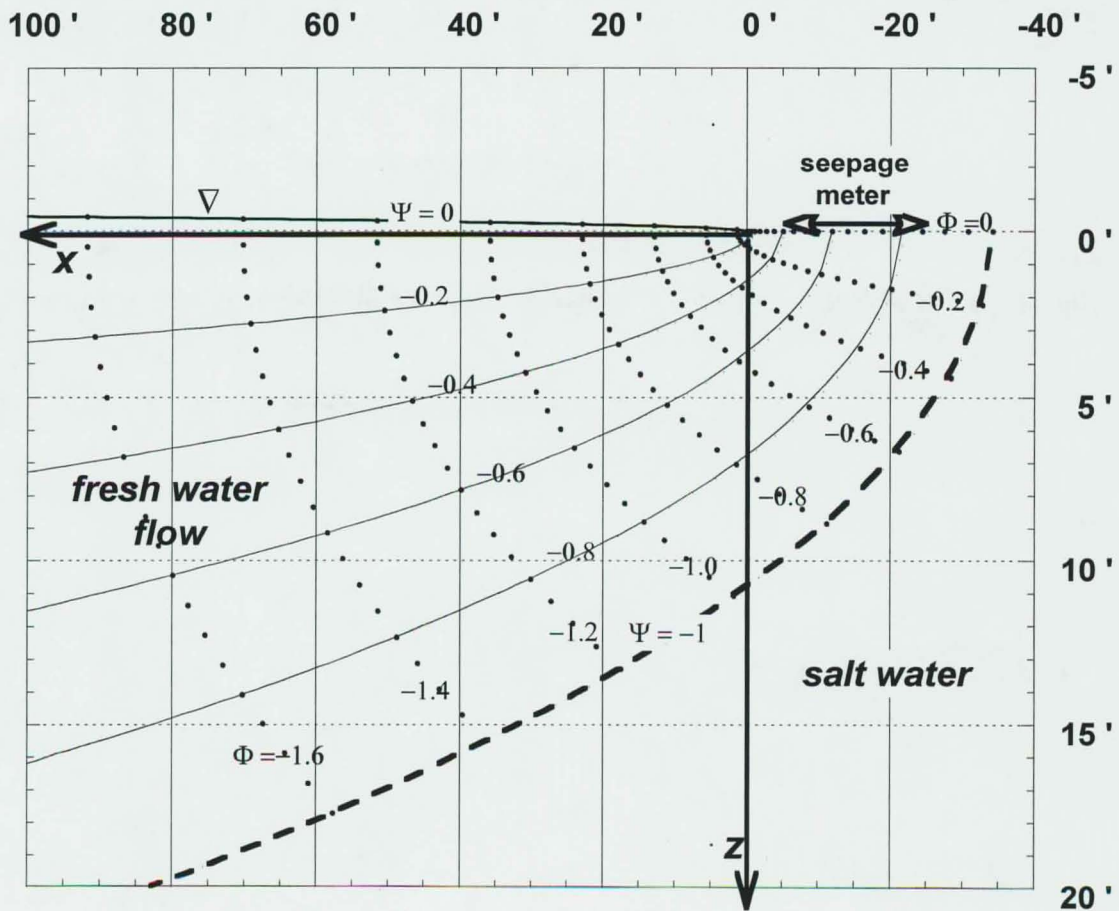


Figure 6. Flow net for the upper glacial aquifer in the vicinity of our study area. The equipotential and stream lines are shown as dotted and solid lines respectively.

It should be emphasized that data on the fresh-salt water interface are continually being collected, and therefore the preliminary model presented here will be refined in the future taking into account the more comprehensive data base. Nevertheless, the theoretical prediction is in reasonable agreement with the currently available data.

To our knowledge, the influence of tidal variation has not been considered by previous theoretical models. Here we will extend Rumner and Shiau's (1968) theory to account for tidal effects. In previous models for saltwater intrusion, it is implicitly assumed that the origin (i.e. intersection of the water table with the coast) is stationary. The cyclic variation of tidal stage is neglected, and the origin is approximated by the mean position between high and low tides. In this study, we will assume that the flow net changes with time. Specifically we will model the tidal effect by using equations (3a) and (3b) to describe the flow at any given instant, but we allow the origin to shift horizontally in synchronization with the tidal cycle. In our study area, this horizontal movement is modeled as a sinusoidal oscillation with an amplitude of $\pm 10'$ (about the mean tidal mark). As indicated in Figure 6, the seepage meter (which was stationary at a fixed location on the seepage face) would oscillate in time between the limiting positions of $X = -5'$ (at low tide) and $X = -25'$ (at high tide) in this non-stationary coordinate system.

Using our model in conjunction with Darcy's law, we derived theoretically the vertical and horizontal components of the specific discharge in the unconfined aquifer as follows:

$$q_x = -K_x \frac{\partial h}{\partial x} = -K_x \frac{\partial}{\partial x} \left(\frac{-\Phi Q}{K_z} \right) = \frac{K_x}{K_z} Q \frac{\partial \Phi}{\partial x} \quad (4a)$$

$$q_z = -K_z \frac{\partial h}{\partial z} = -K_z \frac{\partial}{\partial z} \left(\frac{\Phi Q}{K_z} \right) = Q \frac{\partial \Phi}{\partial z} \quad (4b)$$

Since the potential function $\Phi (= 0)$ is constant for all values of X along the seepage face (Figure 6), the horizontal flow $q_x = 0$ according to equation (4a). In other words, the flow is vertical

coming out of the seepage surface, and combining equations (3) and (4) we arrive at the following prediction for the seepage velocity:

$$q_z = \frac{K_z}{(G+1)\Psi + 1} \quad (5)$$

This theoretical prediction is compared with our seepage measurement in Figure 7, assuming $K_x = 60'$ /day and $K_z = 1.5'$ /day, which are considered to be reasonable estimates for the upper glacial aquifer (Soren, 1978). The seepage velocities is predicted to range from 1.5×10^{-5} cm/s (at high tide) to 3.5×10^{-5} cm/s (at low tide).

The low-tide value agrees well with our seepage measurement (Figure 5), but the high-tide value seems to be too fast.

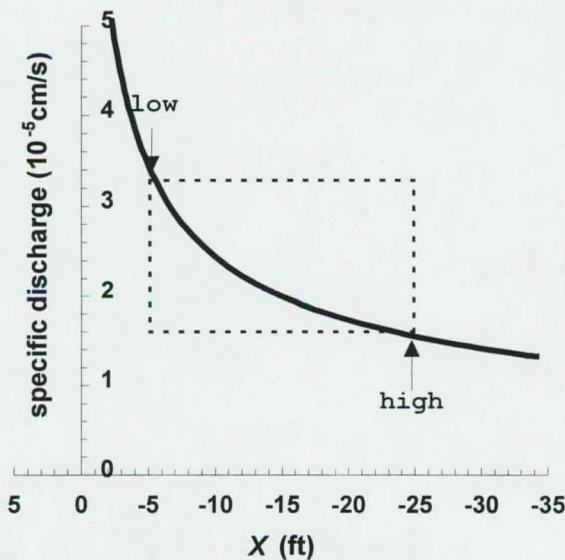


Figure 7. Theoretical prediction of seepage velocity

Acknowledgment

This study of groundwater underflow and the development of the ultrasonic seepage meter was conducted as part of the Peconic Estuary Program (PEP). The authors would like to thank Vito Minea, Suffolk County Department of Health Service's Bureau of Ecology and PEP program manager for supporting this effort. The authors would also like to thank members of the Suffolk County Department of Health Service's Bureau of Water Resources and United States Geological Survey, especially Edward Olson and the well drilling crews for technical support and data collection.

REFERENCES

- Bokuniewicz, H. 1980. Groundwater seepage into Great South Bay, New York. *Estuarine and Coastal Marine Science*. v. 10 pp. 437-444.
- Carr, M.R. and T. C. Winter. 1980. An annotated bibliography of devices developed for direct measurement of seepage. USGS Open-file Report 80-344, Denver, Co. 38pp.
- Cherkauer, D.A. and J.M. McBride. 1988. A remotely operated seepage meter for use in large lakes and rivers. *Groundwater*. v.26 pp. 799-805.
- Church, T. M., 1996. An underground route for the water cycle. *Science*, 380, pp. 579-580, 1996.
- Cooper, H.H., F.A. Kouout, H.R. Henry, and R.E. Glover. 1964. Seawater in coastal aquifers. USGS Water Supply Paper 1613-C, 84pp.
- Fetter, C. W. Jr., *Applied Hydrogeology*, 2nd Edition, Merrill Publishing Company : 149-157 p.
- Fukuo, Y. 1991. Studies on groundwater seepage in Lake Biwa. *Japanese Journal of Hydrological Sciences*. v.21, pp. 93-102.
- Glover, R.E., 1959. The pattern of fresh-water flow in a confined coastal aquifer. *Journal of Geophysical Research*. 64(4) pp. 457-459
- Isrealson, O.W. and R.C. Reeve. 1944. Canal lining experiments in the delta area, Utah. *Agr. Exp. Sta. Rech. Bull.* 313. 52pp.
- Lee, D.R., 1977. A device for measuring seepage flux in lakes and estuaries. *Limnology and Oceanography* 25(1) pp. 140-147.

Paulsen, R.J. and C.F. Smith. 1997. Development of ultrasonic groundwater seepage meter, In preparation.

Rumer, R. R., Jr. And J. C. Shiau. 1968. Saltwater interface in a layered coastal aquifer, *Water Resour. Res.*, 4(6) , 1235-1247 p.

Shaw, R.D. and E.E. Prepas. 1989. Anomalous short term influx of water into seepage meters. *Limnology and Oceanography* 34(7) pp. 1343-1351.

Shaw, R.D. and E.E. Prepas. 1990. Groundwater-lake interactions: I. Accuracy of seepage meter estimates of lake seepage. *Journal of Hydrology*. v.119, pp. 105-120.

Soren, Julian, 1978, Hydrological conditions in the Town of Shelter Island, Suffolk county, Long Island, New York: U.S. Geological Survey Water Resources Investigation 77-77. 22p.

Taniguchi, M. and Y. Fukuo. 1993. Continuous measurement of groundwater seepage using an automatic seepage meter. *Groundwater* 31(4) pp675-679.

Walthall, H.G. and W.G. Reay. 1993. Groundwater seepage meter. NASA Tech Briefs. Dec, 1993. p. 52.